

Article

Depth Spatial Characterization of Marine Environmental Noise in the Zengmu Basin

Xiaoming Cui ^{1,2}, Siyuan Cang ¹, Chao Li ¹, Danling Tang ¹, Qing Hu ² and Huayong Yang ^{1,*}

¹ Southern Marine Science and Engineering Guangdong Laboratory (Guangzhou), Guangzhou 511458, China

² School of Ocean Engineering and Technology, Sun Yat-Sen University, Zhuhai 519000, China

* Correspondence: yanghy@gmlab.ac.cn

Abstract: Based on the measured data obtained from an array of optical fiber hydrophones, this paper analyzes and interprets the depth spatial spectrum characteristics, correlation characteristics, and vertical directionality of marine environmental noise in the Zengmu Basin. The analysis is conducted within the frequency range of 20 Hz to 2500 Hz. Additionally, the statistical characteristics of the probability density distribution of environmental noise in the Zengmu Basin were studied and analyzed. The findings indicate that the predominant ambient noise in the low-frequency range (less than 400 Hz) in the Zengmu Basin is primarily attributed to distant sources, commonly identified as ship radiation noise. In the high-frequency band (greater than 400 Hz), the marine ambient noise is primarily derived from the sea surface, predominantly in the form of wind-generated noise. In the frequency range of 25–1600 Hz, examined in this study, the power spectral density exhibits an average decrease of over 3 dB and a maximum decrease of over 5 dB with each doubling of frequency. When the frequency is below 400 Hz, there is a higher vertical spatial correlation to ambient noise. The vertical directivity of the noise energy is horizontal, meaning that it is perpendicular to the vertical array direction. Additionally, the probability distribution of the noise level approximately follows the Burr distribution. When the frequency exceeds 400 Hz, there is a low vertical spatial correlation to noise. The vertical directivity of environmental noise exhibits distinct grooves in the horizontal direction, and the probability distribution of the noise spectrum level generally follows a normal distribution.



Citation: Cui, X.; Cang, S.; Li, C.; Tang, D.; Hu, Q.; Yang, H. Depth Spatial Characterization of Marine Environmental Noise in the Zengmu Basin. *J. Mar. Sci. Eng.* **2023**, *11*, 2226. <https://doi.org/10.3390/jmse11122226>

Academic Editor: Rouseff Daniel

Received: 3 November 2023

Revised: 16 November 2023

Accepted: 21 November 2023

Published: 24 November 2023



Copyright: © 2023 by the authors. Licensee MDPI, Basel, Switzerland. This article is an open access article distributed under the terms and conditions of the Creative Commons Attribution (CC BY) license (<https://creativecommons.org/licenses/by/4.0/>).

Keywords: marine environmental noise; spectrum characteristics; probability distribution; depth spatial correlation; vertical directionality

1. Introduction

Marine environmental noise is a constant background factor in the underwater acoustic channel. Its sources are diverse, including the movement of seawater, the impact of wind and atmosphere on sea surface noise, changes in water layers due to movement or melting, alterations in submarine geological structures, sounds produced by marine organisms, and noise generated by man-made sources [1–5]. There are differences in marine environmental noise under different time and space conditions [6–10], which makes it extremely difficult to predict marine environmental noise [11,12]. Based on a large amount of data from environmental noise surveys, previous studies have derived empirical prediction formulas and conclusions that are applicable within a specific range [13,14]. On the one hand, marine environmental noise is a disruptive factor that needs to be taken into account when designing and using sonar equipment [1,5]. It is also a type of noise that marine organisms are unable to avoid [15,16]. In order to study and master the spatio-temporal and frequency characteristics of marine environmental noise, it is necessary to conduct a comprehensive investigation and analysis of marine environmental noise [17]. On the other hand, marine environmental noise carries a significant amount of information about the marine environment, which can be analyzed and studied [18,19]. This analysis can provide

internal characteristics such as seabed and water body information, saving considerable manpower and resources compared to direct measurements [20,21]. For a long time, marine environmental noise has been the focus of hydroacoustics research.

As early as the 1940s, Knudsen et al. conducted an analysis of the ambient noise in the Atlantic Ocean and other sea areas during World War II. They summarize the characteristics of marine ambient noise in the range of 100 Hz to 25 kHz, and provide the results of the spectrum characteristics of marine ambient noise in sea states 0 to 6 [2]. However, accurately estimating the sea state itself poses a significant challenge. In 1962, Wenz conducted a study that built upon Knudsen's research, further modifying and expanding upon Knudsen's findings. Wenz's study involved the analysis of experimental data collected at sea. Wenz provided a summary of the Wenz noise spectrum level diagram, highlighting its practical significance [3]. This diagram presents a comprehensive overview of reference noise spectrum levels across various frequency bands, while also identifying the primary sources of noise. As can be seen from the Wenz noise spectrum results, when the frequency is between 50 and 300 Hz, the noise primarily originates from distant shipping radiation noise. In the frequency range of 500 Hz and 10 kHz, the ambient noise in the marine environment exhibits a strong correlation with the velocity of the wind. The Knudsen curve and Wenz curve are distinctive patterns of ambient noise in the ocean, which have been documented and analyzed in various representative studies. Subsequent studies on the characteristics of marine ambient noise are primarily conducted using these patterns.

At present, studies on the characteristics of marine ambient noise have consistently concluded that wind noise and distant shipping noise are considered to be the most significant components of ambient noise in the open sea area. Among them, the ambient noise in the frequency band of 10–300 Hz is mainly caused by the noise source of distant ships, while the primary source of ambient noise from 500 Hz to 20 kHz is wind noise [22]. Harrison [14] and Urick [1] proposed different empirical formulas for wind shutter noise levels based on various sound principles and experimental data. Piggott [6] analyzed the experimental data from shallow waters off the east coast of Canada and derived a semi-empirical formula that correlates wind noise intensity with the logarithm of wind speed. Kuperman et al. [23] measured and calculated the spectrum level of marine ambient noise after removing noise signals from nearby ships in shallow waters. The experimental results showed that the spectrum level of wind noise remained relatively constant regardless of the receiving depth. T.C. Yang et al. [24] calculated the vertical directionality of marine ambient noise in shallow seas using cross-spectral density matrix simulation. Lin Jianheng et al. [25] conducted a long-term observation of ambient noise and sea surface wind speed in the sea area near Qingdao to study the correlation between the noise level and the logarithm of wind speed. Da Lianglong et al. [26] measured ambient noise data in the South China Sea for three months using latent markers. They analyzed the spectral characteristics of the noise and the characteristics of wind clearance noise in typical sea areas. Li Yuhong et al. [27] processed the marine ambient noise data obtained from ASIAEX in 2001 and studied the spatial correlation of marine ambient noise affected by long-range and short-range ship radiation noise. Rouseff et al. [28] combined the acoustic propagation model with the shallow water internal wave model, analyzed and verified the model using measured data, and concluded that internal waves significantly affect the horizontal variations in the noise field. Yang Qiulong et al. [29] analyzed the depth distribution, empirical fitting, probability density distribution, and other statistical characteristics of the measured deep-sea ambient noise in the southern waters of the South China Sea during summer and winter. Shi et al. [30] conducted a 21-month long-term monitoring of ambient noise data in the northeast region of the South China Sea. They analyzed and studied the changes in ambient noise levels during different seasons and at different times of the day and night. Additionally, they analyzed and discussed the characteristics of wind speed and its influence on ambient noise. Jiang et al. [31] analyzed the characteristics of radiated noise from merchant shipping in the Yellow Sea of China. They established a model for the

source level of modern merchant shipping-radiated noise and improved the accuracy of predicting low-frequency marine ambient noise.

Due to the inherent randomness of marine ambient noise, analyzing its spatial and statistical characteristics has always been a focal point and challenge in the study of marine ambient noise. The experimental location of this study is in the Zengmu Basin, which has a flat seabed and a water depth of less than 200 m [32], and this area is also rich in oil and gas resources in the South China Sea. At present, there have been no public reports on the research regarding the spatial characteristics of ambient noise in this area. This paper presents experimental measurement data that offer a relatively ideal description of the characteristics and levels of sea ambient noise in the Zengmu Basin area. This relatively ideal external environment can be ascribed to the limited disruption caused by sailing activities in the vicinity of the measurement site; at the same time, data collection is conducted during optimal sea conditions, which include favorable wind speeds and wave conditions. Based on the ambient noise data recorded during a sea test in the Zengmu Basin, this paper examines the spatial characteristics of ambient noise in the frequency band of 20–2500 Hz. This involves analyzing the spatial spectrum characteristics, correlation, and directionality of the ambient noise field. The characteristics of the probability density distribution of ambient noise levels are statistically analyzed, and the results of fitting three probability distributions to the measured noise levels are provided. The research results of this paper provide references and technical support for underwater target detection and the application research of marine ambient noise in shallow seas.

2. Materials and Methods

2.1. Study Area and Measurement Method

In March 2021, we measured the ambient noise in the Zengmu Basin of the South China Sea. The experimental location and measurement method are shown in Figure 1. The 32-element optical fiber hydrophone array was suspended using the ship's side method to measure the ambient noise. The water depth at the location of the array was measured to be 103 m. The hydrophones in the array were positioned at intervals of 1 m within a range of water depths from 44 m to 75 m. The first hydrophone, designated as H1, is situated at the uppermost section of the array, approximately 44 m below the sea surface. H32 denotes the 32nd hydrophone, positioned at the lowermost part of the array, with a distance of 28 m from the seafloor. During the experimental procedure, the diesel engine was intentionally deactivated to mitigate any potential interference caused by ship noise. However, the generator and certain equipment remained operational throughout the measurement process. To mitigate the effects of drift resulting from ocean currents, a 10 kg anchor block was affixed to the rear end of the array.

The vertical array is a piece of self-developed equipment with a cable diameter of 36 mm, which consists of 32-element low-current-noise fiber optic hydrophones. The average sound pressure sensitivity of the array hydrophones is -145.5 dB (re 1 rad/ μ Pa) within the frequency range of 20 Hz–5 kHz, exhibiting a fluctuation range of less than ± 1.5 dB. Moreover, the cross talk between each array hydrophone and channel is below -50 dB. The hydrophone is fully directional and operates at a sampling frequency of 32.5 kHz. Before the experiment, a SBE911 self-contained thermosalinity depth instrument was used to collect the temperature, salinity, and depth measurements of the array placement position. As shown in Figure 2, based on temperature and salinity measurements, we obtained sound speed profiles by using an empirical formula [1].

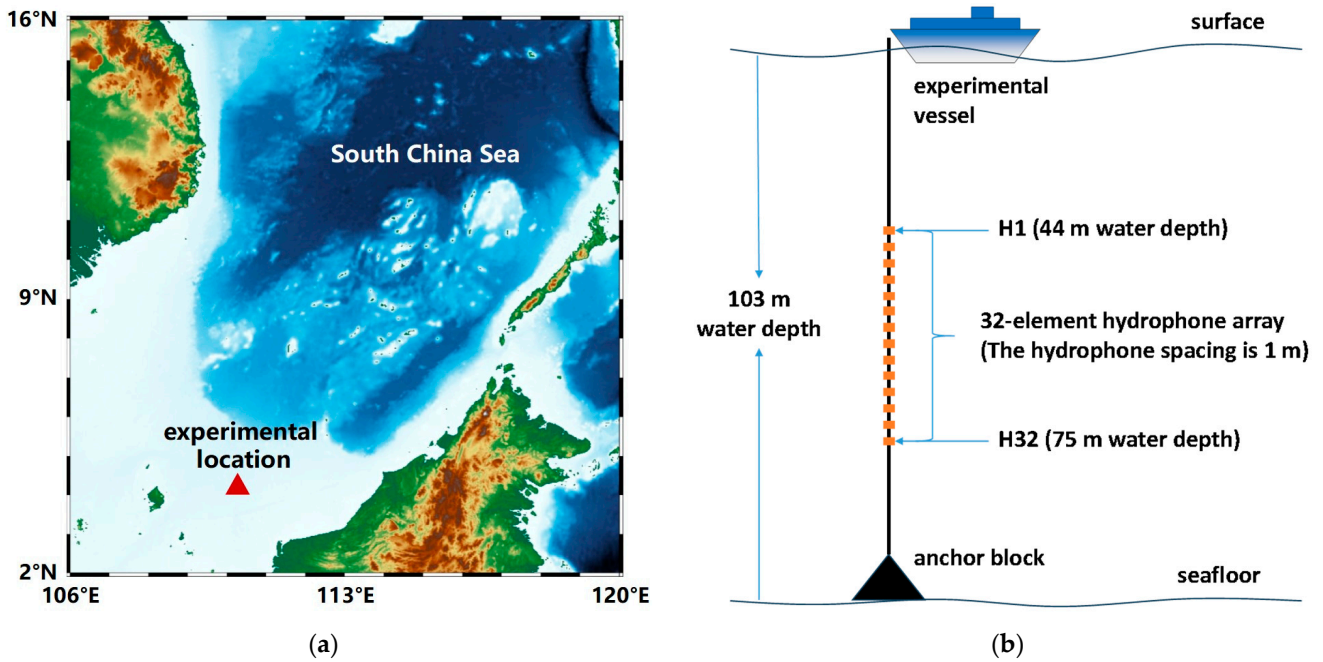


Figure 1. Experimental location and measurement method: (a) the experimental location in the southern South China Sea; (b) the vertical array of a 32-element optical fiber hydrophone.

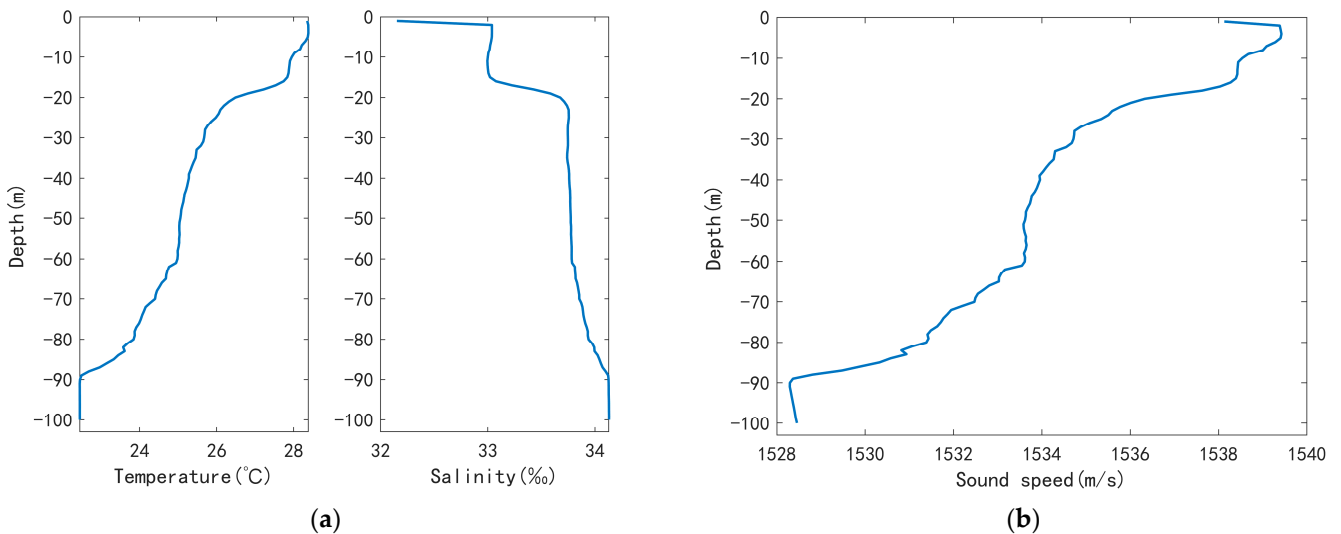


Figure 2. Temperature, salinity, and sound speed profile at the experimental location: (a) the temperature and salinity measurements; (b) the calculated sound speed profile.

It can be seen from Figure 2 that the maximum sound speed is 1539 m/s, corresponding to a depth of 4 m. The minimum sound speed is 1528 m/s, corresponding to a depth of 90 m. Due to the influence of sunlight, a negative sound speed gradient profile is formed in the water column from a depth of 4 m to 90 m.

2.2. Research Methods

When analyzing the noise power spectrum, we select the L discrete signal $x_l[n]$, $l = 1, 2, \dots, L$ of ambient noise, statistically average the power spectrum within a specific bandwidth, Δf_{HL} , and calculate the average power spectrum level (unit: dB) as follows:

$$NL(f_i) = 10\lg \left[\frac{1}{L} \sum_{l=1}^L |P_{l,i}|^2 \right] - M_v - D, i = 1, 2, \dots, N \tag{1}$$

where

$$|P_{l,i}|^2 = \frac{1}{N \cdot M} \frac{2}{\Delta f_{HL}} \sum_{i'=n_1}^{n_2} |X_{l,i'}|^2, N \geq M$$

$$\Delta f_{HL} = f_H - f_L$$

$$f_H = (n_2 - 1)f_s/N, f_L = (n_1 - 1)f_s/N$$

where $X_{l,i'}$ represents the spectrum obtained by performing fast Fourier transform (FFT) on the noise $x_l[n]$, f_s denotes the sampling frequency, M represents the number of data points in the noise signal, and N indicates the length of the FFT. f_H and f_L represent the upper and lower bounds of the narrow band, respectively. f_l denotes the center frequency of this bandwidth spectrum, while M_v represents the sensitivity of the hydrophone. Lastly, D signifies the magnification of the receiving system. The spectrum level of ambient noise is obtained by calculating the index of each data point separately.

The spatial correlation of ambient noise is defined as the average of the product of noise signals received through two different hydrophones at a certain distance in space. The method for calculating the spatial correlation coefficient of a noise field is as follows: First, extract the noise time series Δt_i , which has the same time length as n within the period $x_i(\Delta t_i, z_1), x_i(\Delta t_i, z_2), i = 1, 2, \dots, n$. Then, perform a Fourier transform to obtain $X_i(f, z_1), X_i(f, z_2), i = 1, 2, \dots, n$. In order to minimize the potential impact of random noise source characteristics on the calculation results, the normalized noise interrelation number of n periods is obtained and averaged. The calculation formula is as follows:

$$C(z_1, z_2) = \frac{1}{n} \sum_{i=1}^n \frac{X_i(f, z_1)X_i^*(f, z_2)}{\sqrt{X_i(f, z_1)X_i^*(f, z_1)}\sqrt{X_i(f, z_2)X_i^*(f, z_2)}} \tag{2}$$

where $*$ represents conjugation.

Vertical directionality is one of the typical spatial characteristics of marine ambient noise. It refers to the power of the noise received by hydrophones at various glancing angles, and the glancing angle represents the angle between the noise incident direction and the seabed. Vertical directionality reflects both the directional characteristics of the noise source and the propagation characteristics of marine ambient noise. The formulation for calculating the vertical directionality of the measured ambient noise is shown as follows:

$$B(\theta) = \left| \overline{\sum_{m=1}^M X_{z_m}(f)e^{-iz_mk \sin \theta}} \right|^2 \tag{3}$$

In the formula, $X_{z_m}(f)$ represents the frequency domain signal received by the m array hydrophone with a bandwidth of 1 Hz. The horizontal line at the top indicates the average processing results of multiple periods. z_m represents the depth of the hydrophone, while θ represents the angle between the arrival direction of the sound wave and the normal direction of the array: $-90^\circ \leq \theta \leq 90^\circ$. The angular interval is calculated as 1° , k denotes the wave number $2\pi f/c$ (with c as the sound speed), m as the array number, and M as the total number of array hydrophones. For ease of comparison, the normalized $B(\theta)$, obtained using the formula mentioned above, can provide the vertical directionality of the measured environmental noise after normalization.

2.3. Research Data

In order to accurately obtain the marine ambient noise in the experiment area, we select the data of the measurement period at 19:00 in the evening of 26 March 2021. Three hours before and after the measurement period, the sea conditions were good. As shown in Figure 3a, the sea surface wind speed was approximately 1.05 m/s, and the wave height was around 1 m. Figure 3b illustrates the number of vessels located horizontally within

a 50 km radius from the vertical array. The information regarding the quantity of vessels is obtained from AIS data. The wind speed and wave height data in the experimental sea area were exported from the EAR5 reanalysis data set, which made up for the lack of observation of environmental factors in the experiment.

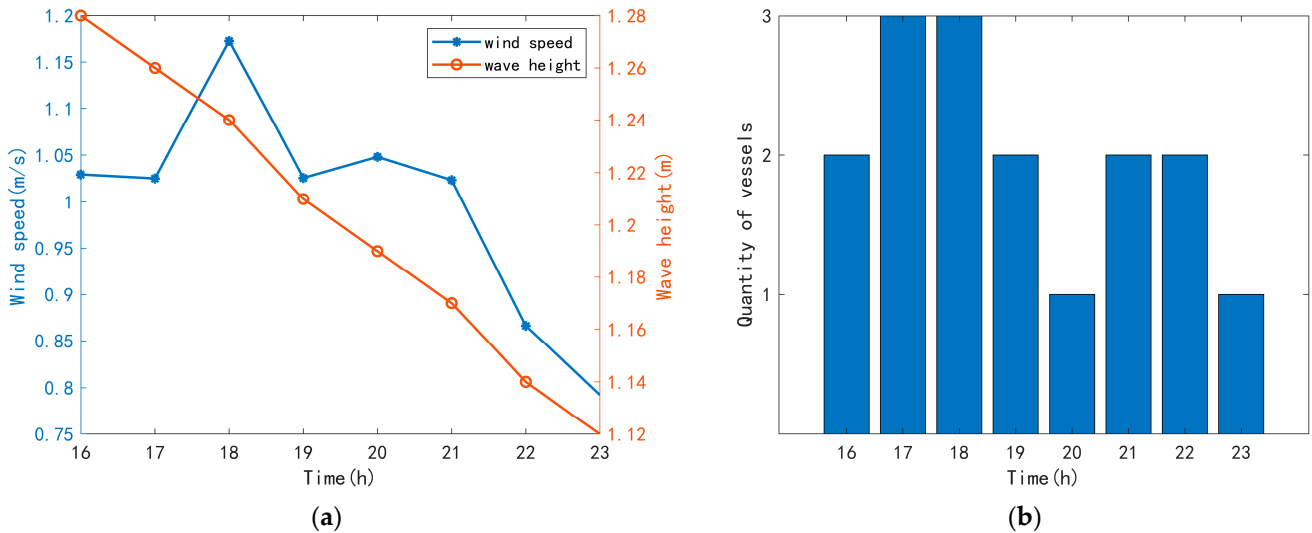


Figure 3. The environmental factors of the experimental location: (a) the wind speed and wave height from the EAR5 reanalysis data set; (b) the quantity of vessels within 50 km of the experimental location.

We filter out the interference noise in the noise spectrum calculation procedure. This paper primarily focuses on analyzing the spatial characteristics of ambient noise in the frequency band of 20–2500 Hz. Figure 4a displays the power spectral density (PSD) of noise for a set of six array hydrophones. The PSD was obtained using the Welch method and the hydrophones were positioned at the top, middle, and bottom of the array. Figure 4b displays the noise levels at various frequency points of the array hydrophones.

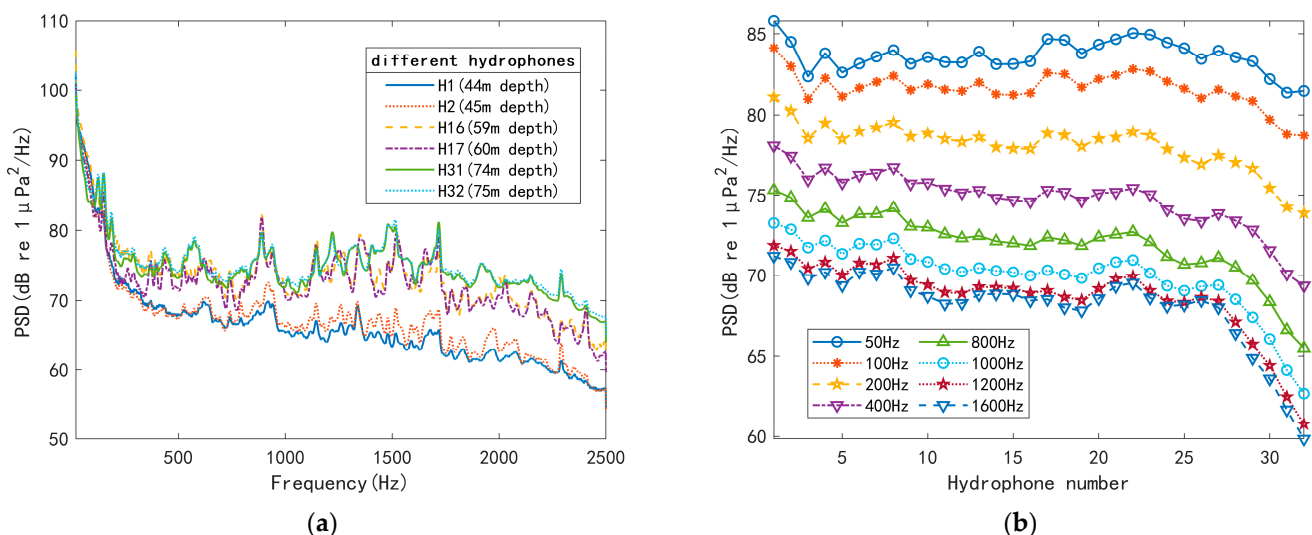


Figure 4. Spectrum processing results of the array hydrophones: (a) PSD of the hydrophones at different depths; (b) the noise levels at various frequency points of the array hydrophones.

In the process of noise measurement, the main engine of the research ship was turned off, but the power generation system was still operational. Figure 4a plots the PSD results of the six selected hydrophones. It can be seen that the PSDs of hydrophones at different depths exhibit interference line spectra. As a result, the noise measured through the array

hydrophones was affected by interference noise from the ship. These discrete line spectrum noises must be mitigated during the computation of the overall sound level. It can also be noticed from Figure 4a that the PSDs of the array hydrophones close to the seafloor (H31 and H32) are significantly higher than those of the array hydrophones close to the surface (H1 and H2) in almost the whole frequency band. Additionally, the noise levels of the hydrophones located in the middle of the array of hydrophones (H16 and H17) are slightly lower than that of the hydrophone array near the seabed. The aforementioned phenomenon is also evident in the findings of Figure 4b. Five frequency points within the analysis band range of 20–2500 Hz have been selected for examination in this paper. The increase in layout depth is observed to result in an increase in the noise level of the hydrophone array at the five frequency points.

The hydrophone array utilized in this experiment employs a zero-buoyancy design. After the stern hanging array is submerged in the water, it lacks the commonly employed lead block to ensure the vertical alignment of the array. According to prior empirical evidence, the 10 kg anchor block proves insufficient in achieving the vertical alignment of the array. Consequently, the vertical array exhibits instability in the horizontal direction during the measurement procedure. According to the aforementioned analysis, it can be deduced that the amplitude of oscillation in the array exhibits an increase as the depth increases. Additionally, the hydrophone located at the bottom records a higher level of noise compared to the hydrophone located at the top. The measurement results depicted in Figure 4a,b demonstrate an increasing trend change in the noise spectrum level from the top end to the bottom end of the array. This observation provides an explanation for the observed phenomenon that deeper distribution of the hydrophone array corresponds to higher noise levels.

3. Results and Discussion

3.1. Depth Spatial Spectrum Characteristics of Ambient Noise

The hydrophone array used for noise measurement is distributed at a water depth range of 44–75 m. In this study, a number of one-third octave frequency points have been chosen for the purpose of processing and analysis. Figure 5a shows the variation in the noise power spectral density with depth. Figure 5b shows the variation in noise levels at three different depths at 1 kHz frequency points over a period of 4 min. Table 1 presents the detailed statistical results of hydrophone noise levels at 10 frequency points across six depths.

Table 1. The noise level of six hydrophones at various depths within the 20–2500 Hz frequency range.

Frequency (Hz)	H1 (dB) 44 m Depth	H2 (dB) 45 m Depth	H16 (dB) 59 m Depth	H17 (dB) 60 m Depth	H31 (dB) 74 m Depth	H32 (dB) 75 m Depth	Mean (dB)	Variance
25	87.36	85.82	84.86	86.81	85.08	85.46	85.90	0.99
50	85.24	83.83	82.55	84.36	81.89	82.30	83.36	1.74
100	82.80	81.55	79.94	81.47	78.14	78.47	80.40	3.46
200	79.08	78.06	76.19	77.35	72.83	72.94	76.08	6.99
400	75.71	74.90	73.00	73.75	68.36	68.07	72.30	10.88
800	73.01	72.35	70.54	70.93	65.13	64.32	69.38	13.88
1000	71.01	70.42	68.65	68.78	62.93	61.65	67.24	15.70
1600	69.96	69.38	67.61	67.61	61.84	60.28	66.11	16.43
2500	69.22	68.63	66.78	66.71	61.00	59.27	65.27	17.10

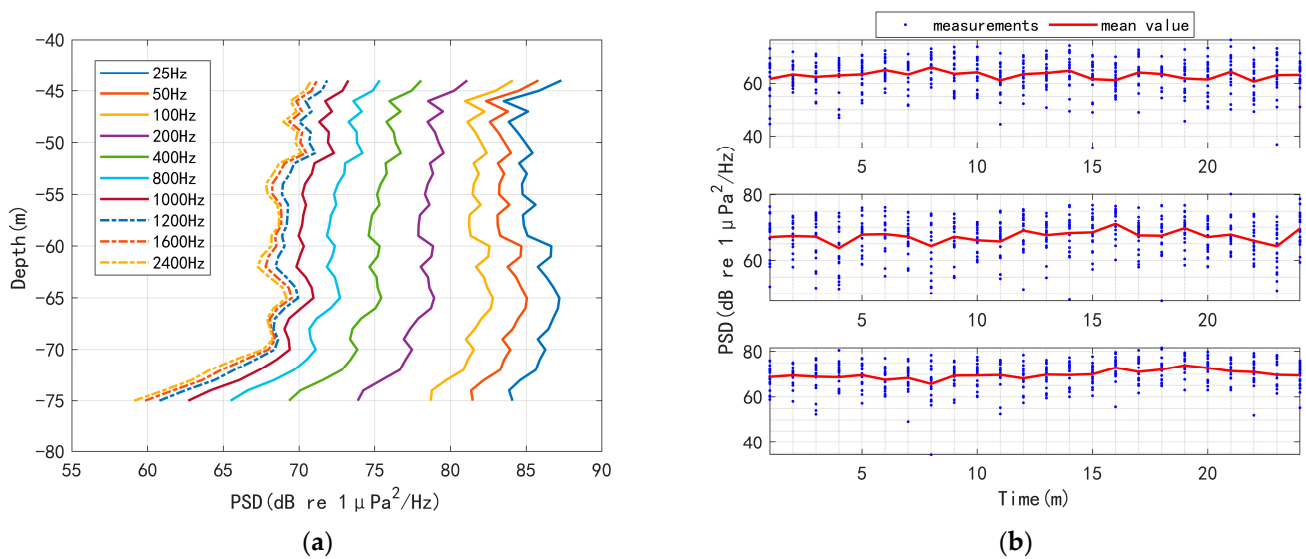


Figure 5. Spectral characteristics of hydrophones with multiple frequencies at different depths: (a) variation in noise levels at different frequencies with depth; (b) variation in noise levels at three different depths with time at 1 kHz frequency point.

It can be seen from Figure 5a that the hydrophone noise power spectral density decreases continuously with the increase in frequency within the measurement depth range. According to the statistical results in Table 1, it can be observed that within the frequency range of 25–1600 Hz, doubling the frequency results in an average decrease of more than 3 dB in the power spectral density, with a maximum decrease exceeding 5 dB. The above processing results are consistent with the noise variation results with depth given in the literature [11]. It can be seen from Figure 5b that the distribution of the noise data is relatively discrete. However, when considering a short time scale and obtaining the average value of the noise data, it is evident that the noise energy changes relatively smoothly over time. In fact, the background noise in the marine environment is essentially a stationary random process. The reason why the distribution of the measured noise data is relatively discrete is that the noise energy changes steadily. The vertical array wobbles horizontally during the experimental measurement. The reasons for the wobbles are analyzed and explained in detail in Section 2.3.

As shown in Figure 5a, the noise power spectral density exhibits a decreasing trend as the depth increases, particularly for frequencies above 400 Hz. It is noteworthy that the reduction amplitude is significantly amplified beyond a depth of 60 m. It can be seen from the calculation in Table 1 that when the frequency exceeds 400 Hz, the average power spectrum drop is approximately 9 dB within the depth range measured experimentally (44–75 m water depth). When the frequency is less than 400 Hz, the average reduction in the power spectrum is less than 5 dB, which is approximately half of the reduction observed at frequencies greater than 400 Hz. It is generally believed that when the frequency is greater than 400 Hz, the noise mainly comes from the wind noise of the sea surface. This portion of the noise energy propagates vertically from the sea surface to the seafloor and attenuates rapidly as the propagation distance increases. As a result, the power spectral density of noise decreases significantly with increasing depth, and the energy of the noise exhibits a downward convergence trend. This is consistent with the results of the noise field variation with depth as reported in the literature [12]. The noise power spectral density below 400 Hz does not change significantly with depth. This is because this portion of the noise energy primarily consists of noise radiated by distant ships, which affects the vertical array as plane waves. The energy distribution of this noise is relatively uniform at each depth, resulting in minimal changes in the noise power spectral density.

In addition, we can see from Table 1 that the sample variance of noise data obtained through the three deep hydrophones at the top, middle, and bottom of the array increases as the frequency increases. The main reason for this phenomenon is that the radiation angle of the noise energy, which plays a major role, gradually changes from the horizontal direction in the far field to the vertical direction in the near field. The higher the frequency of the noise, the faster the sound wave energy attenuates. This results in an increase in the variance in the sample data obtained with the vertically spaced hydrophones as the frequency increases. Because the length of the 32-element hydrophone array does not cover the entire water depth, the experiment does not provide information on the noise spectrum distribution near the sea surface and the seafloor.

Marine environmental noise sources mainly come from far-field ship radiation noise and near-field wind-generated noise. These two noise sources are distributed across different frequency bands, and the transition limit is typically between 300 and 400 Hz. According to the Wenz noise spectrum curve in the literature [4], the level of high-band noise in the spectrum is primarily determined by sea surface wind noise. In order to better explain the characteristics of the ambient noise spectra in the Zengmu Basin, this paper selects the 1 kHz noise level as the reference frequency to analyze the characteristics of marine environmental noise across different frequencies. The empirical relationship between the marine environmental noise spectrum level and the noise spectrum level at the reference frequency is generally expressed as follows:

$$NL(f) = a \times NL_{f_0} + b \quad (4)$$

In Equation (4), a, b are fitting curve coefficients, where a represents the slope and b represents the slope distance. Figure 6 shows the fitting results of the inter-frequency characteristics of low-frequency (100 Hz, 200 Hz) and high-frequency (800 Hz, 1600 Hz) noise spectrum levels, as well as the 1 kHz spectrum levels, at a water depth of 45 m (hydrophone H2).

It can be seen from Figure 6a that the fitting results of the noise spectrum levels at low frequencies of 100 Hz and 200 Hz with 1 kHz are weak. The measured noise data are dispersed to a large extent, and there is no clear linear relationship between them. As can be clearly seen from Figure 6b, the fitting effect between the noise spectrum level and the 1 kHz spectrum level is very good at high frequencies of 800 Hz and 1600 Hz. The measured noise data are concentrated around the fitting line with a small degree of dispersion, indicating a definite linear relationship between the two. This is because the high-frequency marine environmental noise is primarily caused by wind noise on the sea surface, which is consistent with the noise source at 1 kHz. Therefore, there is a strong linear relationship. The low-frequency noise is primarily caused by distant ship radiation, which leads to relatively scattered noise spectrum data. Additionally, the noise spectrum level at 1 kHz exhibits a weak linear relationship. In order to conduct a more comprehensive analysis and elucidate the distinctive features of the aforementioned noise spectrum, Table 2 presents the coefficient of determination (commonly referred to as R-squared) and the root mean square errors (RMSE) derived from the linear fitting results. This analysis is performed to establish the relationship between the noise spectrum levels at various frequency points and the noise spectrum levels at 1 kHz for three depth hydrophones in the vertical array.

It is well-established that a higher R-squared indicates a better linear fitting result and a stronger correlation between the two variables. In Table 2, it can be observed that below 1 kHz, the R-squared of the linear fitting results gradually approaches one as the frequency increases. However, after reaching 1 kHz, the R-squared starts to decrease as the frequency continues to increase. However, as the frequency is increased to 2500 Hz, the R-squared for the fitting results remains significantly higher compared to the low-frequency range (below 400 Hz). Simultaneously, it is evident from Table 2 that for frequencies below 1 kHz, the RMSE of the linear fitting result gradually approaches zero as the frequency increases. After surpassing a frequency of 1 kHz, the RMSE gradually increases as the frequency continues to rise. The aforementioned findings indicate that wind-generated noise predominantly

affects the high-frequency range (above 400 Hz), while also exhibiting a broad bandwidth within this range. Based on the aforementioned analysis, it is evident from Table 2 that the R-squared and RMSE of the linear fitting results for the high-frequency-band noise spectrum level and the 1 kHz noise spectrum level are closer to 1 and 0, respectively, when compared to the low-frequency band. This finding strongly suggests that the marine ambient noise in the Zengmu Basin aligns more closely with the Wenz noise spectrum level curve. Specifically, it indicates that the primary source of low-frequency-band noise originates from distant ships. The high-frequency-band noise is primarily influenced by the noise generated by wind on the surface of the sea.

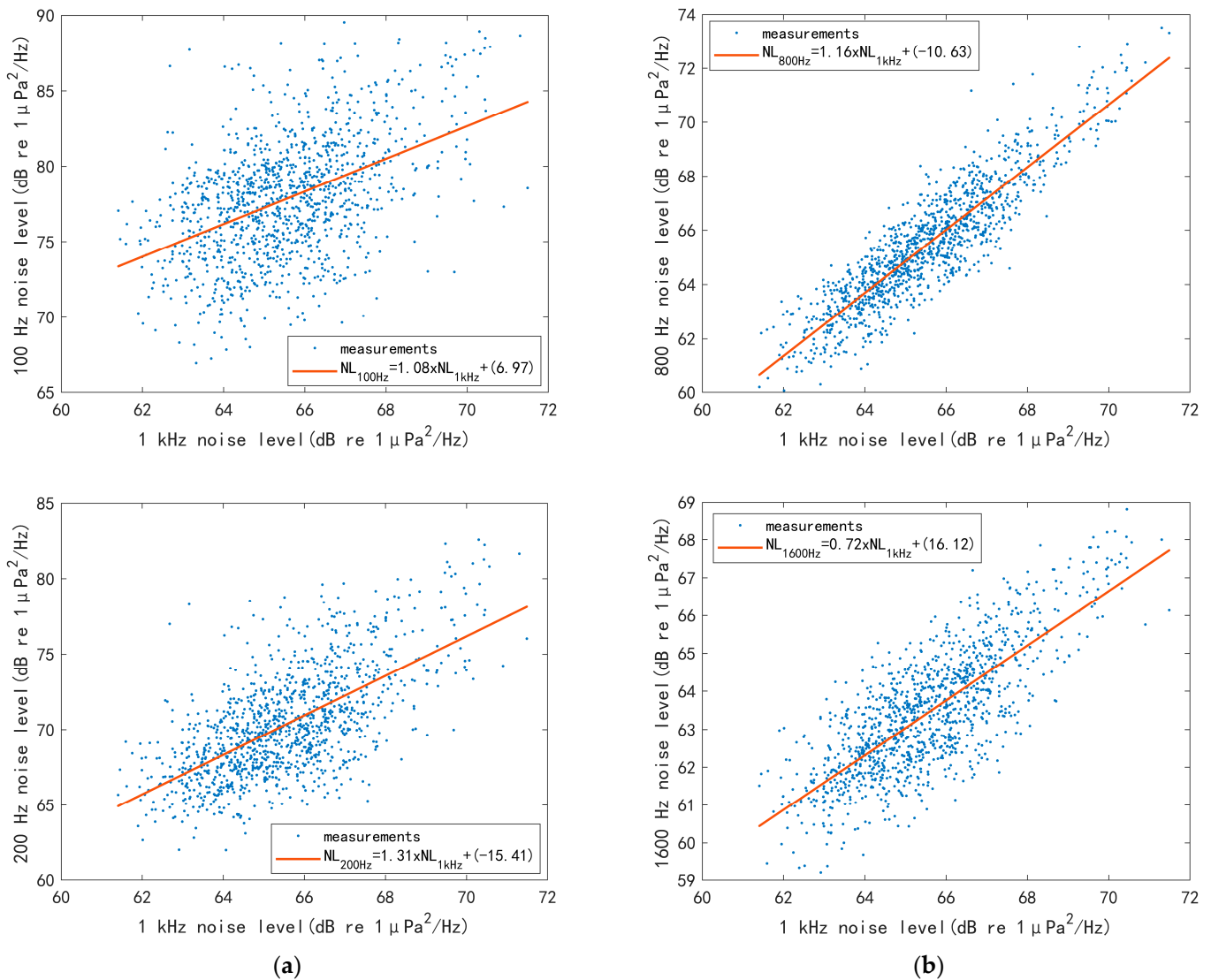


Figure 6. Comparison of fitting results between noise spectrum level and 1 kHz spectrum level: (a) low-frequency band (100 Hz, 200 Hz); (b) high-frequency band (800 Hz, 1600 Hz).

3.2. Spatial Correlation of Ambient Noise

With array hydrophone H1 (44 m water depth) as the reference, Figure 7a, respectively, shows the variation in the spatial correlation coefficient of marine ambient noise with the distance between the array hydrophones. Figure 7b shows the variation in the ambient noise spatial correlation coefficient with frequency. It can be seen from Figure 7a that the vertical spatial correlation coefficient of the noise spectrum of hydrophones at different depths decreases with the increase in array spacing. When the frequency is greater than 200 Hz, the decreasing trend is basically the same. As can be seen from Figure 7b, when

the frequency exceeds 100 Hz, the noise correlation coefficient of hydrophones at different depths gradually decreases with increasing frequency. Additionally, the correlation coefficient decreases as the water depth increases. When the frequency is less than 100 Hz, the noise correlation coefficient oscillates. This oscillation is caused by the interference noise from the ship.

Table 2. The R-squared and RMSE of linear fitting results of multiple depth noise spectrum levels across different frequencies and 1 kHz noise spectrum levels.

Frequency (Hz)	Hydrophone H2 (45 m Water Depth)		Hydrophone H17 (60 m Water Depth)		Hydrophone H32 (75 m Water Depth)	
	R-Squared	RMSE	R-Squared	RMSE	R-Squared	RMSE
50	0.09	4.71	0.04	4.22	0.01	3.54
100	0.22	3.45	0.05	2.83	0.04	2.31
200	0.4	2.71	0.01	2.01	0.18	1.37
400	0.6	1.7	0.17	1.48	0.21	1.1
800	0.79	1.01	0.43	0.99	0.53	0.81
1000	1	0	1	0	1	0
1200	0.73	0.83	0.54	0.85	0.57	0.7
1600	0.53	1.09	0.22	1.23	0.18	0.97
2000	0.47	1.38	0.19	1.56	0.12	1.31
2500	0.45	1.81	0.11	1.91	0.08	1.75

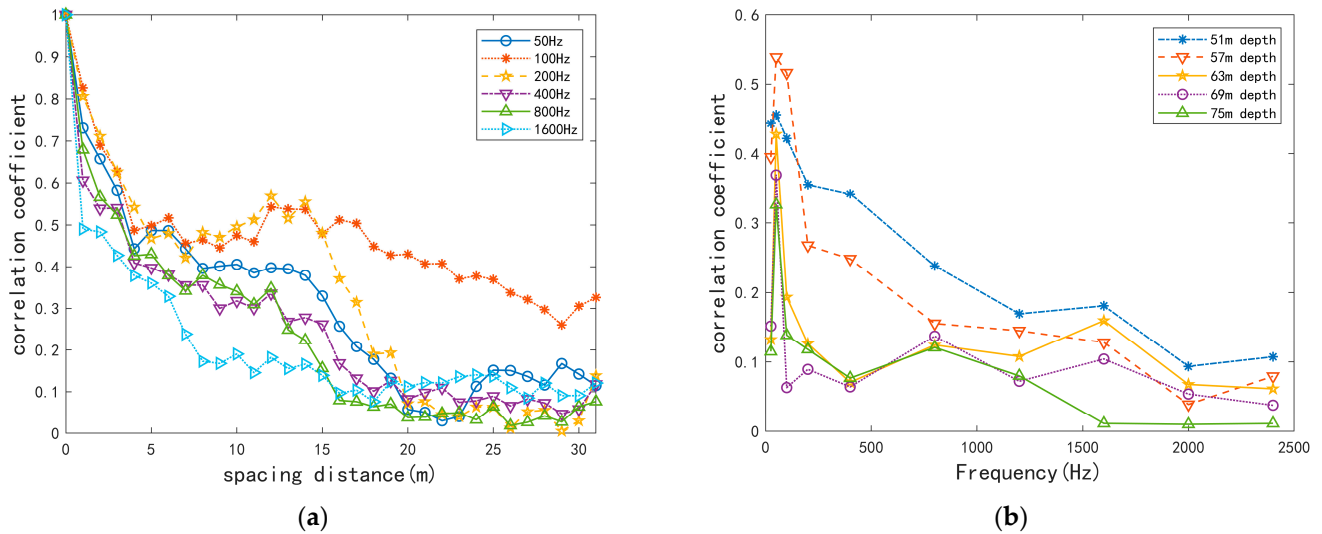


Figure 7. Vertical spatial ambient noise correlation coefficient: (a) variation in the noise spatial correlation coefficient with array spacing; (b) the variation in the noise spatial correlation coefficient with frequency.

We know that the noise received through the vertical array mainly comes from distant shipping radiation noise and the wind-generated noise on the sea surface where the vertical array is located. The noise radiated by distant ships mainly affects the frequency band below 500 Hz. After propagating over long distances, the noise in this part of the wave becomes nearly flat. The wave front of the same order reaches each hydrophone of the vertical array almost simultaneously, with minimal phase variation. Therefore, the noise between the two array hydrophones with a small distance has a high spatial correlation, and the phase difference increases as the array distance increases. The correlation decreases accordingly. The energy distribution of this portion of the noise is also relatively uniform at every depth. Therefore, the noise PSD does not change significantly with depth. However, the hydrophone array primarily collects wind-generated noise from the sea surface in the

frequency band above 500 Hz. The arrival time of this noise varies significantly across different arrays, resulting in a poor spatial correlation of the noise in this frequency band.

3.3. Vertical Directionality of Ambient Noise

Figure 8 shows the vertical directionality of several noise fields at different frequencies. The ordinate is the normalized noise power spectrum of the marine ambient noise measurement period, and the horizontal coordinate is the grazing angle, where 0° is the horizontal direction and 90° is the sea surface direction.

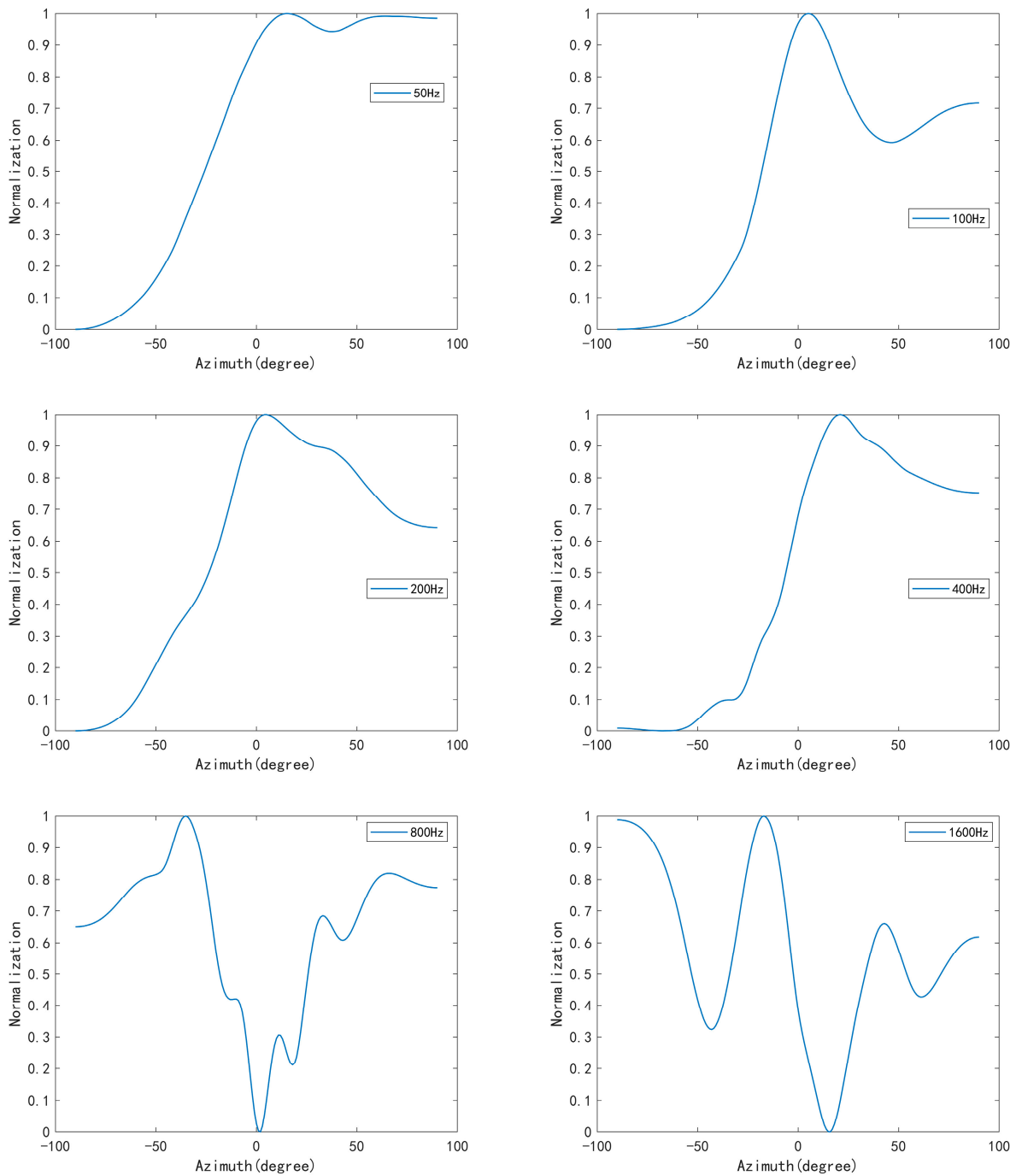


Figure 8. Vertical directionality of noise field.

As can be seen from Figure 8, the noise energy at 100 Hz and 200 Hz is primarily concentrated in the direction near 0° , which is perpendicular to the horizontal orientation of

the receiving array. This noise primarily originates from far-field ship radiation noise. When the frequency exceeds 400 Hz, the energy of the noise field tends to be directed towards the sea surface at a 90° angle. This type of noise is primarily caused by wind noise on the sea surface. When the frequencies are 800 Hz and 1600 Hz, there are noticeable troughs in the range of small grazing angles near the horizontal direction. This phenomenon is commonly observed in shallow sea areas during the summer. The main reason is that the sound wave bends towards the seabed due to the negative gradient of the sound velocity profile. This results in the formation of grooves in the horizontal direction in the vertical directionality of ambient noise. When the frequency is less than 100 Hz, the energy of the noise field is mainly concentrated in the horizontal direction to the sea surface due to the interference noise of the ship. Shan et al. [22] conducted a study in which they performed simulations and experimental analysis to investigate the vertical directionality of environmental noise in islands and reefs. Their findings were found to be highly consistent with the results obtained in this paper regarding the vertical directionality of environmental noise.

3.4. Characteristics of Noise Probability Distribution

Because of the inherent randomness of marine ambient noise, the analysis of its statistical characteristics has always been the primary focus of research in this field. It is pointed out in the literature [2,14] that the probability distribution of marine wind noise levels conforms to the normal distribution law. Based on the normal distribution, Weibull distribution, and Burr distribution, this paper focuses on analyzing the statistical results of the marine ambient noise levels of hydrophones at different depths and multiple frequencies within the frequency range of 100 Hz–2 kHz.

Weibull distribution is commonly used to model the statistical distribution of random variables in the ocean, such as wind speed and wave levels. Its probability density function can be expressed as follows:

$$f(x|A, B) = \begin{cases} \frac{B}{A} \left(\frac{x}{A}\right)^{B-1} \exp\left[-\left(\frac{x}{A}\right)^B\right] & x \geq 0 \\ 0 & x < 0 \end{cases} \quad (5)$$

In Equation (5), A, B represents the undetermined parameter, x represents the random variable, $A > 0$ represents the scale parameter, and $B > 0$ represents the shape parameter. Weibull distribution is related to many other distributions. When $B = 1$, the Weibull distribution is equal to the exponential distribution. For $B = 2$, the Weibull distribution is equivalent to the Rayleigh distribution.

Burr distribution is a family of three-parameter distributions on the positive real line. It can be used to fit a variety of empirical measurement data and is commonly applied in fields such as hydrology and reliability. A wide range of kurtosis and skewness distributions can be achieved by adjusting different parameters. The probability density function of Burr distribution with three parameters can be expressed as follows:

$$f(x|\alpha, c, k) = \frac{\frac{kc}{\alpha} \left(\frac{x}{\alpha}\right)^{c-1}}{\left(1 + \left(\frac{x}{\alpha}\right)^c\right)^{k+1}}, \quad x > 0, \alpha > 0, c > 0, k > 0 \quad (6)$$

In Equation (6), α, c, k are the scale parameters of Burr distribution and the first and second shape parameters, respectively. Figures 9a and 9b, respectively, depict the probability distribution of marine ambient noise levels at multiple frequencies for array hydrophone H2 (45 m water depth) and array hydrophone H17 (60 m water depth). The histogram represents the probability distribution of ambient noise levels in the ocean at each frequency in the experiment. The curve represents the probability fitting results for the corresponding normal distribution, Weibull distribution, and Burr distribution.

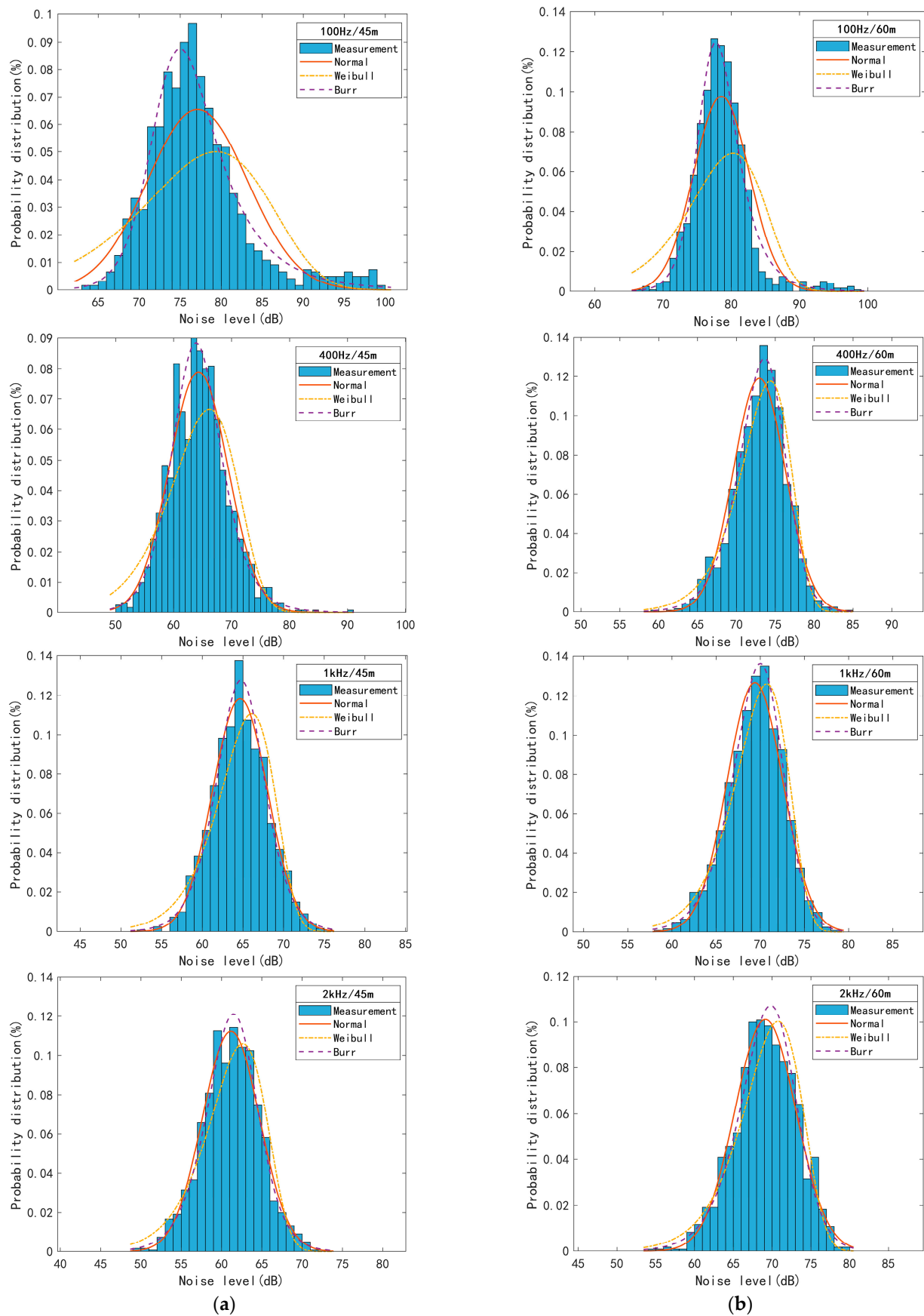


Figure 9. The probability distribution of marine ambient noise at different frequencies for two water depths: (a) 45 m water depth; (b) 60 m water depth.

It can be recognized from Figure 9a,b that the probability distribution of marine ambient noise remains relatively constant at different frequencies at water depths of 45 m and 60 m. In Figure 9a,b, the probability distribution of the 100 Hz noise level approximately follows the Burr distribution. It is also similar to the Chi-square distribution with multiple degrees of freedom or the higher-order normal distribution mixed model. At this time, the spectral level skewness is positive, indicating a left skewness. The probability distribution of noise spectral level above 400 Hz basically follows a normal distribution and is similar to the Burr distribution. The peak value of the Burr distribution is more consistent with the measured noise data at 400 Hz and 1 kHz, while the skewness value of the normal distribution is more consistent with the measured noise data. It is generally believed that in marine ambient noise below 500 Hz, distant shipping noise plays a major role, and this part of the noise component cannot be ignored; ambient noise above 500 Hz is in line with normal distribution, because marine ambient noise in this frequency band is mainly caused by sea surface wind. In this experiment, the wind speed during the measurement period was low and consistently changing. The intensity of the environmental noise generated exhibits a distribution that is relatively close to a normal distribution. This finding is in line with the analysis conducted by Yang et al. [29] on the probability density distribution of noise spectral levels during summer and winter in the southern region of the South China Sea.

4. Conclusions

This paper introduces, for the first time, the experimental data and research results of ambient noise in the depth range of 44–75 m, recorded in the Zengmu Basin; analyzes and explains the spatial spectrum characteristics, correlation characteristics, and vertical direction characteristics of the measured noise in the frequency range of 20–2500 Hz; and analyzes and studies the statistical characteristics of the probability density distribution of ambient noise in the experimental sea area.

We find that the spectrum characteristics of marine ambient noise in the Zengmu Basin exhibit a strong resemblance to the Wenz noise spectrum curve. In the lower frequency range (typically around 300–400 Hz), the predominant ambient noise is primarily attributed to distant shipping radiation noise. Additionally, the noise in this frequency band exhibits a high depth spatial correlation, with the vertical direction of noise energy being perpendicular to the array direction. In the high-frequency band above 400 Hz, the primary source of marine ambient noise is derived from the sea surface, specifically wind-generated noise. Wind-generated noise dominates a broad frequency range and exhibits a low depth spatial correlation in the high-frequency band. The sound line bends towards the seafloor as a result of the negative gradient sound speed profile. This bending causes the environmental noise's vertical directivity to exhibit grooves in the horizontal direction. In addition, the noise power spectral density of hydrophones decreases as the frequency increases at varying depths. In the frequency range of 25–1600 Hz, there is an average decrease of more than 3 dB and a maximum decrease of more than 5 dB in the power spectral density for each doubling of the frequency. Due to external interference, the noise spectrum exhibits a discrete distribution. However, as the observation time is prolonged, the environmental noise spectrum demonstrates the stable characteristics of a stationary random process. By analyzing the statistical characteristics of marine environmental noise, we have discovered that the probability distribution characteristics of noise levels at different depths are similar. When the frequency is less than 400 Hz, the probability distribution of the noise level approximately follows the Burr distribution. Above 400 Hz, the probability distribution of the noise spectrum level essentially follows a normal distribution, but it is also close to the Burr distribution. The peak value of the Burr distribution is more consistent with the measured noise data, and the skewness value of the normal distribution is also more in line with the measured noise data. The research results have significant reference value for the application of sonar in typical sea areas and the analysis of performance and environmental effects.

Author Contributions: Conceptualization, X.C., H.Y., Q.H. and D.T.; methodology, X.C., S.C., Q.H. and H.Y.; validation, S.C. and C.L.; investigation, X.C., C.L., D.T. and H.Y.; data curation, X.C., S.C. and C.L.; writing—original draft preparation, X.C.; writing—review and editing, X.C. and S.C.; visualization, X.C.; supervision, H.Y., D.T. and Q.H.; project administration, X.C. and H.Y.; funding acquisition, H.Y., X.C. and D.T. All authors have read and agreed to the published version of the manuscript.

Funding: This research was supported by the National Key R&D Program of China (2021YFF0501200, 2021YFF0501204), the CAS Key Laboratory of Science and Technology on Operational Oceanography (No. OOST2021-06), the Southern Marine Science and Engineering Guangdong Laboratory (Guangzhou) High-end Talent Program (GML2020GD0801, GML2021GD0810), and the Guangdong Special Support Program (2019BT02H594).

Institutional Review Board Statement: Not applicable.

Informed Consent Statement: Not applicable.

Data Availability Statement: Data are contained within the article.

Acknowledgments: We would like to express our heartfelt thanks for the “South China Sea Ecological Environment Scientific Expedition U1 Voyage”.

Conflicts of Interest: The authors declare no conflict of interest.

References

1. Urlick, R.J. *Ambient Noise in the Sea*; Department of the Navy: Washington, DC, USA, 1984.
2. Knudsen, V.O.; Alford, R.S.; Emling, J.W. Under water ambient noise. *Mar. Res.* **1948**, *7*, 410–429.
3. Wenz, G.M. Acoustic ambient noise in the ocean: Spectra and sources. *J. Acoust. Soc. Am.* **1962**, *34*, 1936–1956. [[CrossRef](#)]
4. Duarte, C.M.; Chapuis, L.; Collin, S.P.; Costa, D.P.; Devassy, R.P.; Eguiluz, V.M.; Erbe, C.; Gordon, T.A.C.; Halpern, B.S.; Harding, H.R.; et al. The soundscape of the Anthropocene ocean. *Science* **2021**, *371*, eaba4658. [[CrossRef](#)] [[PubMed](#)]
5. Guo, X.; Li, F.; Tie, G.; Ma, L. Overview of ocean ambient noise and application prospects. *Physics* **2014**, *43*, 723–731.
6. Piggott, C.L. Ambient Sea Noise at Low Frequencies in Shallow Water of the Scotian Shelf. *J. Acoust. Soc. Am.* **1964**, *36*, 2152–2163. [[CrossRef](#)]
7. Širović, A.; Wiggins, S.M.; Oleson, E.M. Ocean noise in the tropical and subtropical Pacific Ocean. *J. Acoust. Soc. Am.* **2013**, *134*, 2681–2689. [[CrossRef](#)] [[PubMed](#)]
8. Gehrmann, R.A.S.; Barclay, D.R.; Johnson, H.; Shajahan, N.; Nolet, V.; Davies, K.T.A. Ambient noise levels with depth from an underwater glider survey across shipping lanes in the Gulf of St. Lawrence, Canada. *J. Acoust. Soc. Am.* **2023**, *154*, 1735–1745. [[CrossRef](#)]
9. Mo, X.; Wen, H.; Yang, Y.; Zhou, H.; Ruan, H. Statistical characteristics of under-ice noise on the Arctic Chukchi Plateau. *J. Acoust. Soc. Am.* **2023**, *154*, 2489–2498. [[CrossRef](#)]
10. Schwock, F.; Abadi, S. Statistical analysis and modeling of underwater wind noise at the northeast pacific continental margin. *J. Acoust. Soc. Am.* **2021**, *150*, 4166–4177. [[CrossRef](#)]
11. Possenti, L.; Reichart, G.-J.; de Nooijer, L.; Lam, F.-P.; de Jong, C.; Colin, M.; Binnerts, B.; Boot, A.; von der Heydt, A. Predicting the contribution of climate change on North Atlantic underwater sound propagation. *PeerJ* **2023**, *11*, e16208. [[CrossRef](#)]
12. Ma, B.B.; Nystuen, J.A.; Lien, R.-C. Prediction of underwater sound levels from rain and wind. *J. Acoust. Soc. Am.* **2005**, *117*, 3555–3565. [[CrossRef](#)] [[PubMed](#)]
13. Walker, S.C. A model for the spatial coherence of arbitrarily directive noise in the depth-stratified ocean. *J. Acoust. Soc. Am.* **2012**, *131*, EL388–EL394. [[CrossRef](#)] [[PubMed](#)]
14. Harrison, C.H. Formulas for ambient noise level and coherence. *J. Acoust. Soc. Am.* **1996**, *99*, 2055–2066. [[CrossRef](#)]
15. Ogawa, M.; Kimura, S.S. Variations in echolocation click characteristics of finless porpoise in response to day/night and absence/presence of vessel noise. *PLoS ONE* **2023**, *18*, e0288513. [[CrossRef](#)] [[PubMed](#)]
16. Tran, D.D.; Huang, W.; Bohn, A.C.; Wang, D.; Gong, Z.; Makris, N.C.; Ratilal, P. Using a coherent hydrophone array for observing sperm whale range, classification, and shallow-water dive profiles. *J. Acoust. Soc. Am.* **2014**, *135*, 3352–3363. [[CrossRef](#)] [[PubMed](#)]
17. Ragland, J.; Schwock, F.; Munson, M.; Abadi, S. An overview of ambient sound using Ocean Observatories Initiative hydrophones. *J. Acoust. Soc. Am.* **2022**, *151*, 2085–2100. [[CrossRef](#)] [[PubMed](#)]
18. Lani, S.W.; Sabra, K.G.; Hodgkiss, W.S.; Kuperman, W.A.; Roux, P. Coherent processing of shipping noise for ocean monitoring. *J. Acoust. Soc. Am.* **2013**, *133*, EL108–EL113. [[CrossRef](#)]
19. Harrison, C.H. Separation of measured noise coherence matrix into Toeplitz and Hankel parts. *J. Acoust. Soc. Am.* **2017**, *141*, 2812–2820. [[CrossRef](#)]
20. Harrison, C.H.; Simons, D.G. Geoacoustic inversion of ambient noise: A simple method. *J. Acoust. Soc. Am.* **2002**, *112*, 1377–1389. [[CrossRef](#)]

21. Tollefsen, D.; Dosso, S.E. Bayesian geoacoustic inversion of ship noise on a horizontal array. *J. Acoust. Soc. Am.* **2008**, *124*, 788–795. [[CrossRef](#)]
22. Shan, Y.; Lin, J.; Yi, X.; Jiang, P.; Sun, J.; Li, N. Vertical distribution and vertical directionality of ocean ambient noise in waters with islands and reefs. *Acta Acoust.* **2021**, *46*, 1114–1123.
23. Kuperman, W.A.; Ferla, M.C. A shallow water experiment to determine the source spectrum level of wind-generated noise. *J. Acoust. Soc. Am.* **1985**, *77*, 2067–2073. [[CrossRef](#)]
24. Yang, T.C.; Yoo, K. Modeling the environmental influence on the vertical directionality of ambient noise in shallow water. *J. Acoust. Soc. Am.* **1997**, *101*, 2541–2554. [[CrossRef](#)]
25. Lin, J.; Chang, D.; Ma, L.; Li, X.; Jiang, G. Estimation of surface wind speed by ocean ambient noise. *Acta Acoustica* **2001**, *3*, 217–221.
26. Da, L.; Wang, C.; Lu, X.; Han, M.; Deng, X. The characteristic analysis of ambient sea noise spectrum based on submersible buoy. *Acta Oceanol. Sin.* **2014**, *36*, 54–60. (In Chinese)
27. Li, Y.; Yang, Y.; Wen, H.; Cheng, Z. Spatial correlation of ambient noise affected by ship-radiated noise in shallow sea. *J. Appl. Oceanogr.* **2018**, *37*, 120–128.
28. Rouseff, D.; Tang, D. Internal wave effects on the ambient noise notch in the East China Sea: Model/data comparison. *J. Acoust. Soc. Am.* **2006**, *120*, 1284–1294. [[CrossRef](#)] [[PubMed](#)]
29. Yang, Q.; Yang, K.; Ma, Y. Statistical characteristic analysis of ambient noise in deep sea of southern South China Sea. *J. Harbin Eng. Univ.* **2020**, *41*, 1419–1428.
30. Shi, Y.; Yang, Y.; Tian, J.; Sun, C.; Zhao, W.; Li, Z.; Ma, Y. Long-term ambient noise statistics in the northeast South China Sea. *J. Acoust. Soc. Am.* **2019**, *145*, EL501–EL507. [[CrossRef](#)]
31. Jiang, P.; Lin, J.; Sun, J.; Yi, X.; Shan, Y. Source spectrum model for merchant ship radiated noise in the Yellow Sea of China. *Ocean. Eng.* **2020**, *216*, 107607. [[CrossRef](#)]
32. Han, B.; Zhao, Z.; Wang, X.; Sun, Z.; Li, F.; Zhu, B.; Yao, Y.; Liu, L.; Peng, T.; Long, G. Formation of the Zengmu and Beikang Basins, and West Baram Line in the southwestern South China Sea margin. *J. Oceanol. Limnol.* **2023**, *41*, 592–611. [[CrossRef](#)]

Disclaimer/Publisher's Note: The statements, opinions and data contained in all publications are solely those of the individual author(s) and contributor(s) and not of MDPI and/or the editor(s). MDPI and/or the editor(s) disclaim responsibility for any injury to people or property resulting from any ideas, methods, instructions or products referred to in the content.